

Generalized X-Pol Theory and Charge Delocalization States

Jiali Gao,^{*,†} Alessandro Cembran,[†] and Yirong Mo[‡]

Department of Chemistry, Digital Technology Center, and Supercomputing Institute, University of Minnesota, Minneapolis, Minnesota 55455, and Department of Chemistry, Western Michigan University, Kalamazoo, Michigan 49008

Received June 2, 2010

Abstract: The mixed molecular orbital and valence bond (MOVB) method has been used to generalize the explicit polarization (X-Pol) potential to incorporate charge delocalization resonance effects in the framework of valence bond theory. In the original X-Pol method, a macromolecular system is partitioned into individual fragments or blocks, and the molecular orbitals of the system are strictly localized within each block. Consequently, these block-localized molecular orbitals (BLMOs) are nonorthogonal across different blocks. In the generalized X-Pol (GX-Pol) theory, we construct charge delocalization VB states by expanding the localization space from monomer blocks into pairwise delocalized blocks. Thus, the expansion of the basis space leads to charge delocalization between monomer pairs, and a series of pairwise delocalization states can be constructed. In general, L -body delocalized states can be analogously defined by grouping L monomer blocks into one. The Hartree product wave function for each state can be fully antisymmetrized, which introduces explicitly exchange repulsion among all blocks. The GX-Pol wave function is a linear combination of all L -body charge transfer (valence bond) states, which incorporates charge delocalization and their resonance as well as static correlation effects. The GX-Pol method provides a general and rigorous theory to incorporate charge delocalization explicitly into these fragment-based electronic structural methods for macromolecular systems.

1. Introduction

The explicit polarization (X-Pol) method is the first practical fragment-based molecular orbital^{1–5} approach for macromolecular simulations^{2,6–8} in which a Hartree product wave function is used on the basis of antisymmetric wave functions of individual subsystems. By construction, molecular orbitals in the X-Pol wave function are strictly localized within the subspace defined by each individual block; that is, these are block-localized molecular orbitals (BLMOs). However, the use of a Hartree product wave function neglects exchange repulsion and charge transfer effects between different blocks. Previously, an empirical Lennard-Jones potential was used to account for the repulsive interactions,^{1–5,8} and we have presented an approach to incorporate the exchange

repulsion explicitly into the X-Pol method by antisymmetrizing its wave function.^{9–13} It was found that the total exchange repulsion is short-ranged, as is well-known, and is essentially pairwise additive for two water trimer complexes examined.⁹ The latter is somewhat surprising in view of the need for orthogonalization of the BLMOs. Nevertheless, these findings suggest that the use of pairwise energy terms could be a very good approximation for the treatment of exchange repulsion interactions.

The strict block localization of molecular orbitals within each subsystem in the X-Pol wave function also excludes charge transfer (CT) contributions between different blocks.^{11,14–20} Although the amount of charge transferred is relatively small, the energy component due to CT effects can be significant and it is important in hydrogen-bonded interactions,^{15,20} critical for biomolecular modeling. The inclusion of charge transfer effects in the X-Pol method can be easily accomplished, but it necessarily requires the

* Corresponding author: e-mail gao@jialigao.org.

† University of Minnesota.

‡ Western Michigan University.

expansion of the orbital space of the localization blocks, and a number of approaches can be envisioned. Here, we describe one approach to systematically include CT configurations into a generalized X-Pol (GX-Pol) wave function.

Methods for treating fragmental electronic structures may be traced to the work of McWeeny²¹ or even earlier, who discussed the density matrices of orthogonal group functions; however, Stoll and Preuss²² were the first to describe a procedure based on many-body interaction energy correction to improve the energy of such a fragment molecular orbital approach as an approximation to the Hartree–Fock (HF) or density functional energy:

$$E_{\text{HF}} \approx E_0 + \sum_{ab}^{\text{dimers}} (E_{ab} - E_0) + \sum_{abc}^{\text{trimers}} \Delta E_{abc} + \dots \quad (1)$$

where E_0 is the total monomer energy and the subsequent summations correspond to the dimer, trimer, etc., corrections. The many-body interaction energy correction approach of Stoll and Preuss treats the monomer, dimer, trimer, etc., terms in the electrostatic field of the rest of the system.^{22,23} This is different from the many-body decomposition scheme of Stillinger and co-workers,²⁴ in which the many-body terms do not include polarization by the rest of the system. The energy correction at each order of expansion (dimer, trimer, etc.) is obtained by subtracting the interaction energies of the preceding order, making the computational procedure a fast-converging, build-up approach that is exceedingly simple and straightforward.^{25,26} However, the molecular wave function is not available from such a fragment molecular orbital approach, and the somewhat ad hoc energy addition and subtraction scheme makes it difficult to obtain analytical gradients of the total energy (of course, it is always possible to obtain the gradients by a variety of procedures, at the expense of higher computational costs).⁴ It is important to note that the configuration weights of different many-body terms are not identical, although it is implicitly assumed to be the same in this approach.

In this paper, we use the mixed molecular orbital and valence bond (MOVB) approach to generalize the X-Pol wave function into a multistate X-Pol wave function in the framework of valence bond theory.^{27–33} In the generalized explicit polarization (GX-Pol) wave function, charge transfer as well as exchange repulsion effects can be systematically determined by the self-consistent field (SCF) method for the entire system. Rather than an ad hoc energy correction expansion, the approach is similar to the traditional multi-configuration self-consistent field (MCSCF), and complete-active-space self-consistent field (CASSCF) or equivalently ab initio valence bond self-consistent field (VBSCF) methods,³⁴ applied to treating the resonance of charge transfer VB states. Consequently, static correlation effects are, at least partially, included into the GX-Pol method. In the following, we first present the theoretical background in section 2. Then we summarize the computational details to illustrate the generalized X-Pol method. Results and discussion are given in section 4, followed by a summary of the main conclusions from this work.

2. Method

For completeness, we first briefly outline the “monomeric” X-Pol wave function.^{1–5} Here, we use the phrase “monomer X-Pol” to emphasize that the total molecular wave function of a condensed-phase system including proteins is constructed from monomer wave functions to distinguish it from the generalization to many-body delocalized states to be described below. Then, we introduce the dimeric charge delocalization state to construct a two-body X-Pol wave function and its generalization to many-body X-Pol wave functions. Finally, we propose to employ these charge delocalization states as effective valence bond (VB) configurations in VBSCF optimization.^{27,28,30–32} We emphasize here that although the theory and illustrative examples are given in terms of wave function theory, *the method and algorithm are identically applicable to density functional theory (DFT), by use of block-localized density functional theory (BLDFT) to define VB states, as described in ref 27*. We also discuss the distinction between consistent diabatic configuration (CDC) and variational diabatic configuration (VDC) methods.³²

2.1. Block Localization and the Monomeric X-Pol Wave Function. In the X-Pol method,^{1–5} a macromolecular system is partitioned into M blocks. The a th block contains k_a basis functions and n_a electrons, and there are a total of K primitive basis functions and N electrons in the system:

$$K = \sum_{a=1}^M k_a \quad \text{and} \quad N = \sum_{a=1}^M n_a \quad (2)$$

Molecular orbitals in a given block are written as linear combinations of the primitive basis functions located on atoms in that specific subspace $\{\chi_\mu^a; \mu = 1, \dots, k_a\}$:

$$\phi_j^a = \sum_{\mu=1}^{k_a} c_{j\mu}^a \chi_\mu^a \quad (3)$$

The X-Pol wave function is constructed from the monomer blocks as a Hartree product of the determinant wave functions of individual blocks:¹

$$\Psi_x = R_x \hat{A}(\Phi_1) \hat{A}(\Phi_2) \dots \hat{A}(\Phi_M) \quad (4)$$

where \hat{A} is an antisymmetrizing operator, R_x is the normalization constant, and Φ_a is a successive product of the occupied spin orbitals in the a th subsystem (eq 3):

$$\Phi_a = \phi_1^a \phi_2^a \dots \phi_{n_a}^a \quad (5)$$

For convenience in the following discussion, eq 4 is called the “monomer” X-Pol wave function, which itself can be antisymmetrized as a block-localized wave function (BLW).^{10–13,30,31}

$$\Psi_x^A = R_x^A \hat{A} \left(\prod_a^M \Phi_a \right) \quad (6)$$

The antisymmetrized X-Pol wave function, also known as BLW,¹⁰ includes explicitly the interfragment eXchange interactions (X-Pol-X)⁹ that are ignored in the Hartree

product X-Pol wave function (eq 4) but are approximated empirically by Lennard-Jones terms.^{1–3}

2.2. Charge Transfer (Delocalization) States and Many-Body X-Pol Wave Functions. Since the molecular orbitals (MOs) are strictly block-localized within each subsystem by construction, there is no possibility of charge transfer between different monomer blocks.^{10,11,27} The charge delocalization energy due to intermolecular (or interfragment) charge transfer can be very important for hydrogen-bonding complexes and biomolecular interactions.^{11,15,20,35–39} For example, the energy component due to charge transfer in the dimer complex of water amounts to −0.4 kcal/mol¹¹ of the total hydrogen bonding energy (−5 kcal/mol).⁴⁰ Note that the term charge transfer used here is more rigorously related to electronic delocalization to distinguish it from the diabatic states in electron transfer reaction; however, in this paper, we use both charge transfer and charge delocalization without specific distinction since the method is equally applicable to electron transfer processes. In the monomer X-Pol method (eq 4), charge transfer effects are modeled *effectively* as electrostatic interactions as in molecular mechanics, which is adequate in the spirit of force field development to keep the formalism simple and the computational procedure efficient.^{1–4,8} On the other hand, in situations where the explicit treatment of charge transfer effects is of interest,^{20,27} it is desirable to define a general approach to treat this effect in the X-Pol theory.

To this end, we generalize the monomer X-Pol wave function to dimer, and generally, many-body, X-Pol wave functions. First, we define a charge transfer state between monomers *a* and *b*, whose wave function is written as a Hartree product of the antisymmetric (determinant) wave function of the dimer (*ab*) and the antisymmetric wave functions of all other monomers:

$$\Psi_{(ab)} = R_{(ab)} \hat{A}(\Phi_1) \dots \hat{A}(\Phi_{ab}) \dots \hat{A}(\Phi_M) \quad (7)$$

where $R_{(ab)}$ is the normalization constant for the wave function defined above. Clearly, it is straightforward to define analogously a fully antisymmetrized dimer X-Pol (X-Pol-X) wave function:

$$\Psi_{(ab)}^A = R_{(ab)}^A \hat{A}(\Phi_1 \dots \Phi_{ab} \dots \Phi_M) \quad (8)$$

An important distinction between the wave functions defined by eqs 4 and 7 (and by eqs 6 and 8) is that the molecular orbitals in the dimer, indexed by (ab) , Φ_{ab} , are expanded over the basis functions of the entire dimer space, in contrast to that in eq 4 with strict block localization within each monomer space. Thus, there are $M - 1$ blocks remaining in the state defined by eq 7 (and eq 8) since two blocks are combined to form a single dimeric subsystem. Importantly, since the wave function specified in eq 7 or 8 represents the expansion of basis space, it introduces charge delocalization effects between monomers *a* and *b* in comparison with that of eq 4. The energy difference between these two states (eqs 6 and 8) corresponds to the X-Pol charge transfer energy between the two subsystems according to our interaction energy decomposition analysis (EDA) based on block-localized wave function (BLW):^{11,41}

$$\Delta E_{(ab)}^{\text{CT}} = \langle \Psi_{(ab)}^A | H | \Psi_{(ab)}^A \rangle - \langle \Psi_x^A | H | \Psi_x^A \rangle \quad (9)$$

Consequently, the individual dimer X-Pol wave function in eq 7 (or eq 8) represents a CT state between two monomer blocks, in the presence of the electrostatic field of the rest of the system. We note that, unlike other EDA approaches,^{41,42} the intermediate wave functions at all stages of the decomposition analysis are fully defined and *variationally optimized*,¹¹ providing the most relevant reference states in polarization and charge transfer analysis.^{12,20,43}

We define the total dimeric generalized X-Pol (GX-Pol) wave function as a linear combination of all dimeric charge transfer states:

$$\Theta_{X2} = \sum_{a=1}^M \sum_{b=a+1}^M c_{(ab)} \Psi_{(ab)}^A \quad (10)$$

where the subscript X2 specifies a GX-Pol wave function at the dimer CT level and $c_{(ab)}$ is a configuration coefficient to be optimized along with all the BLMO coefficients in exactly the same fashion as in standard MCSCF or VBSCF methods.^{34,44} In fact, the interpretation of the configuration specified by eq 7, and the fully antisymmetrized counterpart (eq 8), is an effective valence bond state, and eq 10 is a VB wave function defined by these CT states (the valence bond resonance integrals between determinant states are given below). Thus, the generalization of the X-Pol method to the treatment of multiconfigurational states is equivalent to the previously described MOVB theory^{30,31} which has been used in the study of chemical reactions in solution,^{20,28–31} cluster analysis,²⁹ and a range of charge transfer analysis applications.^{12,15–17,20,43,45} MOVB has been presented with the use of ab initio molecular orbital theory,^{28,30–32} semiempirical methods,^{33,46} and density functional theory.²⁷

The ground-state energy of the entire system, including all or some dimeric CT contributions, is minimized by a valence bond self-consistent field (VBSCF) method, which can be expressed as follows:

$$E_{X2} = \langle \Theta_{X2} | H | \Theta_{X2} \rangle \quad (11)$$

A general, many-body X-Pol wave function can be defined similarly. Thus, for a full system separated into M blocks (monomers), the L -body GX-Pol wave function is

$$\Theta_{XL} = \underbrace{\sum_{a=1}^M \sum_{b=a+1}^M \dots \sum_{f=a+L-1}^M}_{L \text{ summation terms}} c_{ab\dots f} \Psi_{(ab\dots f)}^A \quad (12)$$

where the subscript XL denotes the L -body GX-Pol wave function, and the individual effective VB configuration is defined analogously as in eq 7 by grouping L blocks into one delocalized subsystem. Equation 12 defines a full range of many-body GX-Pol wave functions, from the simplest case in which each monomer block is fully separated and the molecular orbitals are strictly block-localized (the monomer X-Pol wave function) to the full delocalization of the entire system, which is the Hartree–Fock result. Of course, it is clear from eqs 10 and 12 that, in contrast to the method of

Stoll and Preuss,²² there is no redundancy to have to determine lower-body states to construct an L -body GX-Pol wave function since the GX-Pol method is not a build-up model and the charge delocalization of the lower-order contributions is fully encompassed in the GX-Pol states. For example, it is not necessary to construct monomer and dimer states to form a “trimer correction” term.

It is of interest to point out that the intermediate VB wave functions, generally defined by eq 12, are multiconfigurational wave functions, and they include partially static correlation effects and dispersion contributions.²⁷ An exploration of this property is of considerable interest and remains for future investigations.

2.3. Consistent and Variational Diabatic Configurations. Previously, we have classified the effective VB states optimized by the VBSCF method as consistent diabatic configurations (CDC) in that the individual VB states, called diabatic configurations, are consistently optimized to yield the minimum ground-state energy.³² An alternative method is to use a configuration interaction (CI) approach to optimize the configuration coefficients in eq 10 with fixed BLMOs in each effective VB state that has been variationally optimized individually.^{28,30–33} We call these VB states the variational diabatic configurations (VDC).³² Obviously, the CDC and VDC states have different energies for the same state defined by eq 7 (and eq 8) since they are obtained by different energy minimization targets.³² In the latter case, one solves the generalized secular determinant equation to yield the configuration coefficients and the ground-state energy:^{27,28,30–32}

$$\begin{vmatrix} H_{11} - ES_{11} & \dots & H_{1,M2} - ES_{1,M2} \\ \dots & \dots & \dots \\ H_{M2,1} - ES_{M2,1} & \dots & H_{M2,M2} - ES_{M2,M2} \end{vmatrix} = 0 \quad (13)$$

where $M2 = M(M - 1)/2$ is the total number of dimer configurations, $S_{(ab),(st)}$ is the overlap matrix between dimer configurations (ab) and (st) , and the Hamiltonian matrix element and VB resonance integral is defined by^{27,30–32,47}

$$H_{(ab),(st)} = \langle \Psi_{(ab)}^A | H | \Psi_{(st)}^A \rangle \quad (14)$$

We note that the explicit expression of eq 14 has been given previously,^{30,31} and again, the approach described here is applicable to both molecular orbital theory and density functional theory as described by Mo et al.¹⁴ and by Cembran et al.²⁷

3. Computational Details

All computations have been performed by use of a locally modified GAMESS program⁴⁸ and the Xiamen University Valence Bond (XMVB) program.³⁴ The valence double- ξ 6-31+G(d) basis set with polarization and diffuse functions was used to optimize the trimer geometries, and the aug-cc-pCVDZ⁴⁹ basis set was used in energy calculations. The goal here is to illustrate the significance of resonance effects by coupling dimeric charge delocalization VB states in the GX-Pol theory. A more thorough examination with a larger set of systems will be published later. The minimum energy configuration of a cyclic water trimer structure, **c-W**₃, along with another trimer configuration, **s-W**₃, which was con-

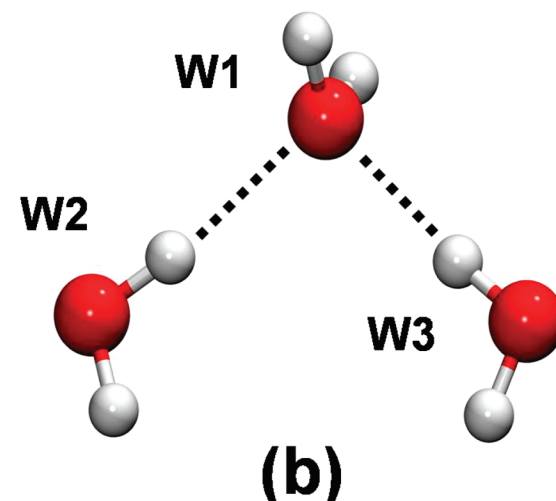
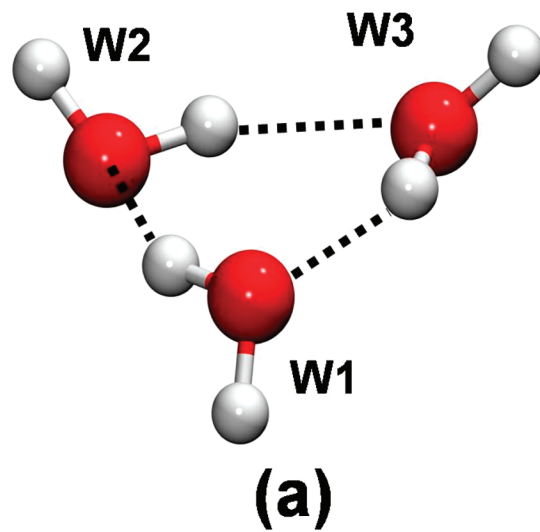


Figure 1. Schematic representation of (a) the minimum water trimer structure (**c-W**₃) and (b) a symmetric configuration (**s-W**₃).

structed by minimizing the dimer water complex first followed by placing a third water molecule at the C_2 image about the bisection of the acceptor water molecule, are adopted in this study. Both structures are depicted in Figure 1.

Throughout the following discussion, each water monomer in the trimer complexes is partitioned as a monomer block, and their geometries are kept as those in the optimized configuration at the HF/6-31+G(d) level. The notation $\Psi_{(ab)}^A = \hat{A}\{\Phi_{ab}\Phi_c\}$, where $a, b, c = 1, 2, \text{ or } 3$, is used to represent a charge delocalization state between water molecules a and b in the electrostatic field of the third water monomer c . We use the fully antisymmetrized wave function that also includes explicitly exchange repulsion between different blocks. To estimate the dimeric charge delocalization energy, the block-localized wave function for the triblock system $\Psi_{\text{X-Pol-X}} = \hat{A}\{\Phi_1\Phi_2\Phi_3\}$ is also determined.⁹ The structural weight is determined as described by Chirgwin and Coulson.⁵⁰

Table 1. Computed Total Energies for the Cyclic Water Trimer Minimum Structure and for a Symmetric Trimer Geometry^a

method	total energy (hartrees)	
	c-W ₃	s-W ₃
$\Phi_1^0 + \Phi_2^0 + \Phi_3^0$	-228.128 79	-228.129 19
Ψ_{123}^{HF}	-228.147 55	-228.139 35
$\Psi_{X\text{-Pol}}^A = \hat{A}(\Phi_1\Phi_2\Phi_3)$	-228.142 58	-228.136 26
$\Psi_{23}^A = \hat{A}(\Phi_{23}\Phi_1)$	-228.144 37	-228.136 34
$\Psi_{13}^A = \hat{A}(\Phi_{13}\Phi_2)$	-228.144 13	-228.137 75
$\Psi_{12}^A = \hat{A}(\Phi_{12}\Phi_3)$	-228.144 31	-228.137 75
VDC-MOVB(3)	-228.145 37	-228.139 09
CDC-MOVB(3)	-228.151 16	-228.141 02

^a All calculations are performed with the aug-cc-pCVTZ basis set at the HF/6-31+G(d) geometry.

Table 2. Computed Relative Energies for the Cyclic Water Trimer Minimum Structure and for a Symmetric Trimer Geometry^a

method	relative energy (kcal/mol)	
	c-W ₃	s-W ₃
$\Phi_1^0 + \Phi_2^0 + \Phi_3^0$	0.00	0.00
$\Psi_{X\text{-Pol}}^A = \hat{A}(\Phi_1\Phi_2\Phi_3)$	-8.65 (0.00)	-4.43 (0.00)
$\Psi_{23}^A = \hat{A}(\Phi_{23}\Phi_1)$	-9.78 (-1.12)	-4.48 (-0.05)
$\Psi_{13}^A = \hat{A}(\Phi_{13}\Phi_2)$	-9.62 (-0.97)	-5.37 (-0.93)
$\Psi_{12}^A = \hat{A}(\Phi_{12}\Phi_3)$	-9.74 (-1.09)	-5.37 (-0.93)
$\Psi_{X\text{-Pol}}^A + \text{CT}$	-11.83 (-3.18)	-6.35 (-1.92)
Ψ_{123}^{HF}	-11.77 (-3.12)	-6.37 (-1.94)
VDC-MOVB(3)	-10.40 (-1.75)	-6.21 (-1.78)
CDC-MOVB(3)	-14.03 (-5.38)	-7.42 (-2.99)

^a All calculations are performed with the aug-cc-pCVTZ basis set at the HF/6-31+G(d) geometry. Values in parentheses are interaction energies due to charge transfer [$\Delta E_{(ab)}^{\text{CT}}$] without basis-set superposition error correction.

4. Results and Discussion

Listed in Tables 1 and 2 are the total and relative energies for the isolated monomers at their complex configurations, the antisymmetrized X-Pol (i.e., X-Pol-X) trimer ($\Psi_{X\text{-Pol-X}}^A$), and the dimeric charge delocalization states [$\Psi_{ab}^A = \hat{A}(\Phi_{ab}\Phi_c)$]. The upper limit of charge transfer interaction energy between a pair of water molecules, in the presence of the third water in the trimer complex, is the energy difference between the two variational diabatic configurations Ψ_{ab}^A and $\Psi_{X\text{-Pol}}^A$. Using these VDC states as the effective VB configurations, one can carry out a configuration interaction calculation by optimizing only the configurational coefficients of the MOVB wave function.^{28,30,31} In this case, the individual charge delocalization states remain unchanged, and thereby the resonance among these states, or the diabatic coupling, is not necessarily optimal. The energy from this procedure (eq 13) is called the VDC-MOVB(3) method, where the number in parentheses indicates the number of configurations used in the VB optimization. Alternatively, MOVB wave function can be fully optimized following standard procedures such as MCSCF and VBSCF methods in which both the orbital and configurational coefficients are simultaneously varied.³² Since the individual CT diabatic states are obtained consistently with the ground-state energy minimization, the result is denoted by CDC-MOVB(3). Here, resonance effects make important contributions.

Table 2 shows that the X-Pol binding energies for the two water trimer complexes, c-W₃ and s-W₃, are -8.65 and -4.43 kcal/mol, respectively, significantly smaller than the fully delocalized HF results (-11.77 and -6.37 kcal/mol). The difference represents the total charge delocalization effects (also called charge transfer in energy decomposition analysis) due to block localization imposed by the X-Pol wave function, which are -3.12 and -1.94 kcal/mol, respectively. The energies due to charge transfer between a pair of water molecules are shown in parentheses, which are in the range of -0.97 to -1.12 kcal/mol for the c-W₃ complex. Apparently, the charge transfer effect between two water molecules is significantly enhanced in the presence of the polarization by the third water in comparison with the water dimer alone, which has a CT energy of -0.2 and -0.4 kcal/mol from the 6-31++G(d,p) and aug-cc-pVTZ basis sets. The pairwise charge delocalization energies are very similar for the three pairs in c-W₃ since each water accepts and donates a hydrogen bond from the other two water molecules. On the other hand, monomers W2 and W3 (Figure 1) are placed in a repulsive orientation in the trimer complex s-W₃, which exhibits little charge transfer effects (-0.05 kcal/mol), which are depicted in Figure 2. These two water monomers (W2 and W3) have a C₂ symmetry about the molecular axis of the central water (W1), which accepts a hydrogen bond from each of the W2 and W3 monomers. The charge transfer energies are -0.93 kcal/mol for each of the two hydrogen bonds.

The resonance effects due to charge delocalization from VDC-MOVB(3) calculations are modest, lowering the X-Pol energy by -1.75 and -1.78 kcal/mol in the two complexes. Specifically, in the cyclic complex, c-W₃, which involves a sequence of donor and acceptor hydrogen bonds, 56% of the total charge delocalization effect is obtained in the configuration interaction approach, suggesting that there is a strong cooperative effect in the overall charge delocalization interaction that is not fully included in the VDC approach. In the case of s-W₃, in which there is little cooperative interaction, 92% of charge delocalization contributions are determined. Full relaxation of the GX-Pol wave function, by simultaneous optimization of both the orbital and configurational coefficients in the CDC-MOVB method, achieves the greatest extent of valence bond resonance effect. The computed total stabilization energies, relative to the monomer X-Pol result, in the two trimer complexes are -5.38 and -2.99 kcal/mol for c-W₃ and s-W₃, respectively, far greater than the total charge delocalization energy at the Hartree-Fock level of theory. The MOVB method is a multiconfigurational approach, which also includes partial static correlation effects; this is reflected by the total electronic energy, lower than the corresponding HF value (Table 1). Thus, of the total stabilization energies in the trimer complexes, -2.2 and -1.1 kcal/mol, the amounts exceeding the corresponding HF binding energies, may be attributed to dispersion correlation effects. For comparison, Schutz et al.⁵¹ estimated that the MP2 contribution to the binding energy of the c-W₃ complex is -3.60 kcal/mol with the HF optimized geometry and the 6-311++G(d,p) basis

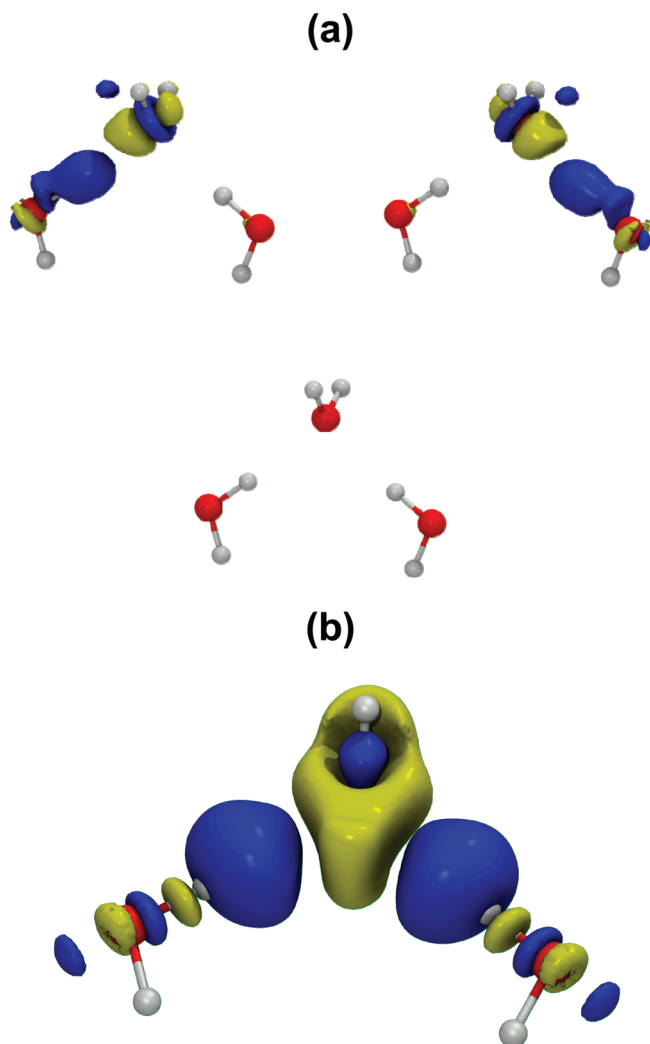


Figure 2. Electron density difference contour between the charge delocalized and the strictly localized systems, $\rho(\hat{A}\psi_1\psi_2\psi_3)$, in the **s-W₃** complex, (a) for the three pairs of dimer charge transfer state, $\rho(\hat{A}\psi_{ab}\psi_c)$, and (b) for the resonance state of the fully delocalized system from the two-body generalized explicit polarization (GX-Pol) wave function, $\rho(\Theta_{X2})$. The structure orientation is shown in Figure 1b and the contour levels are at 0.0002 au with blue contours representing gain in electron density and yellow contours representing charge depletion.

set. The binding energy for the **c-W₃** complex has been estimated to be -15.8 kcal/mol by use of CCSD(T)/CBS.⁴⁰

Table 2 shows that the charge delocalization energies are roughly additive in both cases. In particular, the sum of the X-Pol energy and the total VDC charge delocalization energy ($\Psi_{X\text{-Pol}}^A + \text{CT}$) is very close to the corresponding HF interaction energy. Here, the total charge delocalization energy is the sum of the three pairwise charge transfer contributions (e.g., -3.18 kcal/mol in the **c-W₃** structure). The fast converging property, that is, a monomeric X-Pol calculation followed by a variational dimeric charge delocalization energy correction, in a many-body interaction decomposition scheme²² can be attributed to the fact that the dominant, nonadditive polarization effects¹¹ have already been included in the X-Pol wave function.¹ However, one should be cautious about the seemingly good agreement in this ap-

Table 3. Configuration Weights from the CDC and VDC-MOV_B(3) Wave Functions

configuration	c-W₃		s-W₃	
	CDC	VDC	CDC	VDC
$\Psi_{23}^A = \hat{A}(\Phi_{23}\Phi_1)$	0.384	0.375	0.000	-0.875
$\Psi_{13}^A \hat{A}(\Phi_{13}\Phi_2)$	0.305	0.272	0.500	0.937
$\Psi_{12}^A \hat{A}(\Phi_{12}\Phi_3)$	0.311	0.353	0.500	0.937

proach because the additive CT energy (-3.18 kcal/mol) is greater than the total charge delocalization effect (-3.12 kcal/mol). Note that, inasmuch as the difference is small, the sum exceeds the total charge delocalization energy, without inclusion of correlation contributions, is significant to indicate the nonvariational discrepancy resulting from a lack of consideration of cooperative effects of the entire system. Furthermore, the difference between the VDC and CDC results presented above indicates that good agreement between the additive results and the total HF interaction energies is fortuitous since orbital relaxation is essential in full VBSCF (MCSCF) charge resonance. It appears to be important to further analyze the additive properties on a wider range of structures and functionalities by use of the methods described here.

Nevertheless, in practice, it appears to be a reasonable strategy to use the X-Pol potential with an empirical estimate for the exchange repulsion to carry out Monte Carlo and molecular dynamics simulations of a condensed-phase system,^{1–3,5,8} followed by the pairwise CT and exchange repulsion energy corrections to obtain more accurate results. The most systematic approach is to employ the many-body GX-Pol wave function in CDC-MOV_B calculations to determine the ground-state potential energy surface in dynamics simulations.

The Chirgwin–Coulson structural weights⁵⁰ from MOV_B calculations are given in Table 3 for both trimer complexes. The structural weight can be formulated in a number of ways, and the results in Table 3 are determined as follows:^{34,50}

$$w_{(ab)} = c_{(ab)}^2 + \sum_{(st) \neq (ab)}^3 c_{(ab)} c_{(st)} \langle \Psi_{(ab)}^A | \Psi_{(st)}^A \rangle \quad (15)$$

Obviously, eq 15 should not be confused with the familiar Mulliken population analysis.⁵² The structural weights provide key insight into the nature of chemical bonding in valence bond theory, and are an indication of the resonance contributions of charge delocalization states in the present analysis. In the case of the cyclic configuration, **c-W₃**, the hydrogen-bond strengths are very similar; thereby, both the CDC and VDC methods yield similar structural contributions in the total wave function. However, for the symmetric trimer complex, **s-W₃**, the charge transfer state $\Psi_{(23)}^A$ has negligible contribution to the charge delocalization of the entire system in the CDC-MOV_B wave function. The overlap integrals between $\Psi_{(23)}^A$ and the other two CT states are essentially zero, and the structural weight for $\Psi_{(23)}^A$ is zero. However, the variationally optimized diabatic states are strongly overlapping, with calculated overlap integrals of 0.999 between $\Psi_{(23)}^A$ and two other states. As a result, there is strong out-of-phase mixing in these VDC states. The difference

between the CDC and VDC is a further indication of the lack of cooperative effects in the nonvariational optimization of the total VDC wave function.

Figure 2 illustrates the individual pairwise charge delocalization effects in the electrostatic field of the other monomer and the resonance delocalization results in the GX-Pol wave function for the **s-W₃** trimer complex. The electron density difference (EDD) isosurface^{11,53} is obtained by subtracting the strictly localized, but fully polarized, X-Pol-X electron density from the corresponding delocalized wave functions, for the dimer delocalized pairs (Figure 2a) and for the valence bond resonance state (Figure 2b). In the dimer delocalization states between W1 and W2 and between W1 and W3 (see also Figure 1), electron densities are depleted (yellow contours) from the hydrogen-bond acceptor water (W1), predominantly from oxygen, whereas charge densities are accumulated (blue contours) along the hydrogen-bond donor H–O bond vector, principally located on the hydrogen atom. There is no noticeable charge density variation (the contour level was set to be 0.0002 au) in the W2–W3 delocalization state, consistent with the negligibly small (-0.05 kcal/mol) CT energy. The resonance of these three states, with nearly 50% contributions from the W1–W2 and W1–W3 delocalization states and essentially zero structural weight from the W2–W3 complex, shows the cooperative effect of these states. The charge density loss from the hydrogen-bond acceptor W1 water is spread out over the entire molecule and symmetrized, along with some compensating polarization gains in the inner part of the density distribution. It is interesting to notice the alternating pattern along the donor O–H bonds due to gain in charge density from CT and polarization delocalization along the bond vector. The overall molecular charge delocalization from individual charge transfer states is well represented in the total molecular electron density from the CDC optimization of the GX-Pol wave function.

Figure 3 shows the local two-body charge transfer (CT) in the presence of polarization of the third water, relative to the fully localized monomer state in the cyclic minimum energy complex, **c-W₃**. The resonance delocalization of the three states in Figure 3 determined by the GX-Pol model is depicted in Figure 4a, which is compared with the charge transfer (CT) effects in the fully delocalized HF determinant wave function in Figure 4b. It is aesthetically pleasing to visualize that the traditional Heitler–London–Slater–Pauling valence bond resonance theory of localized configurations as modeled by the GX-Pol method can provide an excellent description of the charge delocalization (i.e., charge transfer) as illustrated by the fully delocalized Hartree–Fock wave function. Importantly, such analyses coupled with quantitative structural weight can provide a deeper understanding of intermolecular interactions, including charge transfer effects in condensed phases.²⁰

5. Conclusions

The explicit polarization (X-Pol) method has been generalized to incorporate charge delocalization resonance effects in the framework of valence bond theory. In the original X-Pol method, a macromolecular system is partitioned into

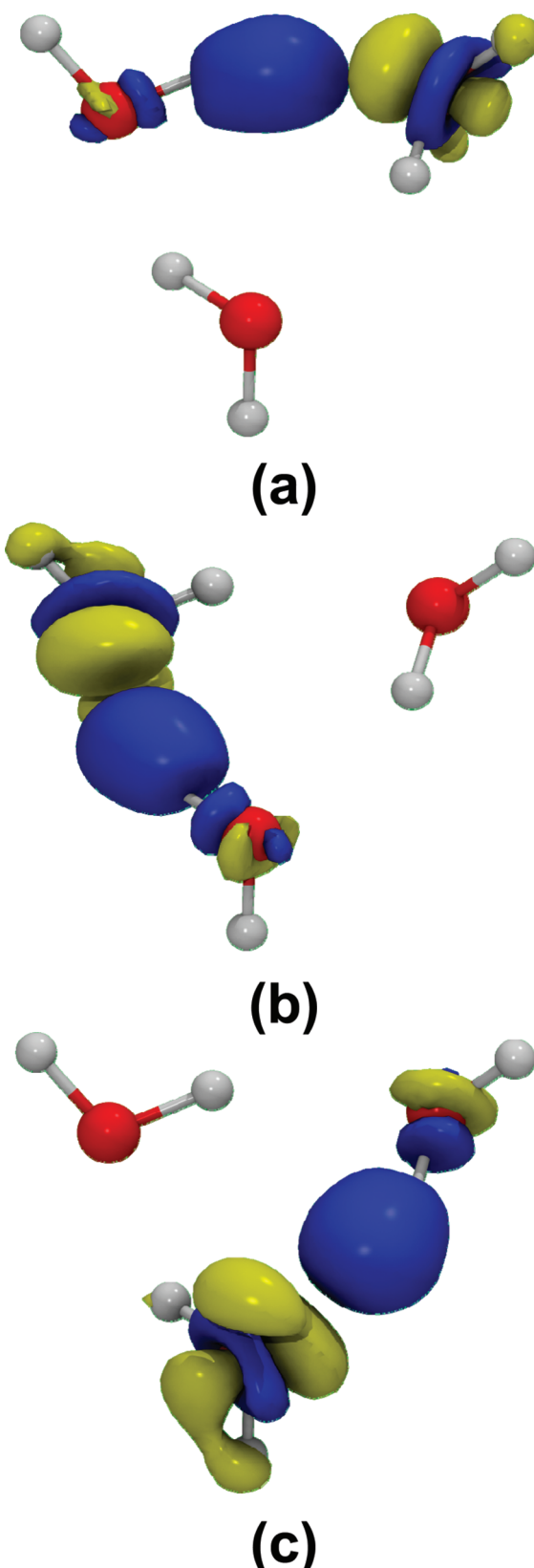


Figure 3. Electron density difference isosurface between the pairwise charge delocalized and the strictly localized system, $\rho(\hat{A}\psi_1\psi_2\psi_3)$, in the **c-W₃** complex: (a) W2–W3 dimer pair, $\rho(\hat{A}\psi_{23}\psi_1)$; (b) W1–W2 dimer pair, $\rho(\hat{A}\psi_{12}\psi_3)$; and (c) W1–W3 dimer pair, $\rho(\hat{A}\psi_{13}\psi_2)$. The structure orientation is shown in Figure 1a and the contour levels are at 0.0002 au, with blue contours representing gain in electron density and yellow contours representing charge depletion.

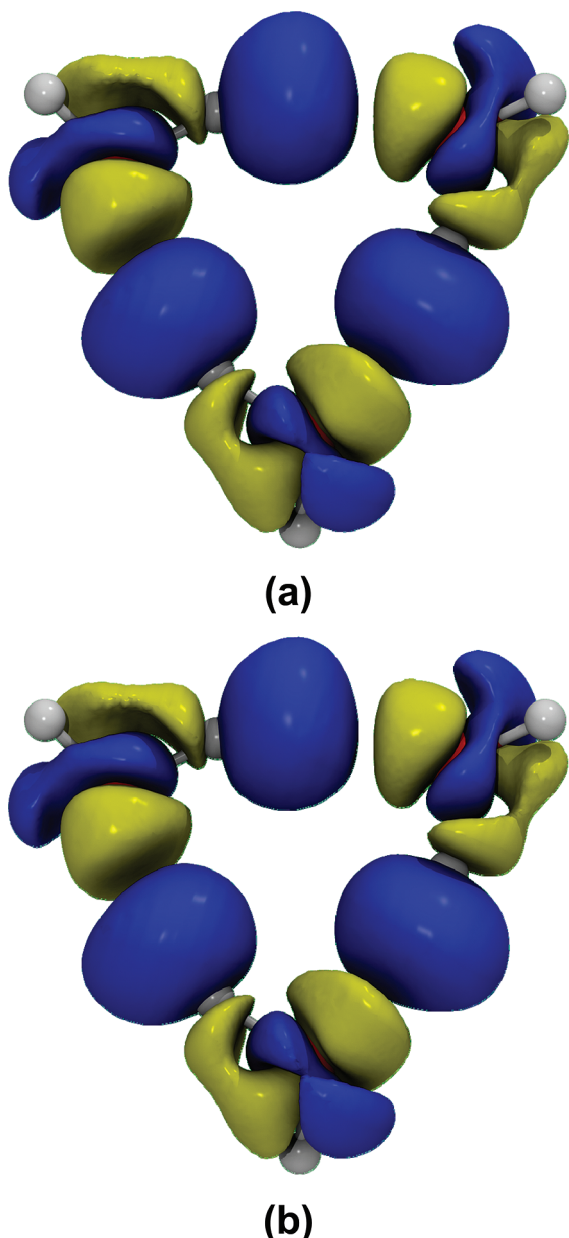


Figure 4. Comparison of (a) resonance charge delocalization modeled by the two-body GX-Pol wave function, Θ_{X2} , for $c\text{-W}_3$, which is a combination of the three states illustrated in Figure 3, and (b) charge transfer effects from Hartree–Fock theory. Electron density difference from the three-block X-Pol-X state, $\rho(\hat{A}\psi_1\psi_2\psi_3)$, is depicted at a contour level of 0.0002 au, with blue contours representing gain in electron density and yellow contours representing charge depletion. Note that the two figures look identical, which is the main point illustrated here.

individual blocks, which may be a single water molecule, a residue, a group of residues and molecules, or a subset of atomic orbitals on the same or different atoms. Molecular orbitals are strictly localized within each block, by virtue of expansion of MOs over basis functions within each subsystem only. Consequently, these block-localized molecular orbitals (BLMOs) are nonorthogonal across different blocks, but they can be orthogonal within each block. The X-Pol wave function is constructed as a Hartree product of the individually determinant wave functions of all blocks, which

means that the exchange repulsion, dispersion correlation, and charge transfer between different blocks are neglected but are approximated empirically in X-Pol.

In the generalized X-Pol (GX-Pol) theory, we construct charge delocalization VB states by expanding the block localization space from individual blocks into pairwise delocalized blocks. Thus, the expansion of the basis space leads to charge delocalization between monomer pairs, and a series of $M \times (M - 1)/2$ pairwise charge delocalization states (which can also be called charge transfer states) can be constructed, where M is the total number of blocks (subsystems). The wave function for each of these CT states is a Hartree product of $M - 1$ blocks since two blocks have been grouped into a single CT unit. In general, L -body delocalized states can be analogously defined by grouping L monomer blocks into one. The Hartree product wave function for each state can be fully antisymmetrized, which introduces explicitly exchange repulsion interactions among all blocks. The GX-Pol wave function is a linear combination of all L -body delocalization VB states, which incorporates charge delocalization and their resonance as well as static correlation effects. The GX-Pol theory is illustrated by considering two water trimer complexes, one with a cooperative hydrogen-bonding network and another consisting of repulsive pair interactions. The illustrative examples show that the GX-Pol method can effectively incorporate charge delocalization and exchange repulsion explicitly in these fragment-based electronic structural methods for macromolecular systems.

Acknowledgment. We are grateful to Dr. Lingchun Song for computational assistance and valuable discussions. This work is supported by the National Science Foundation (Grant CHE09-57162).

References

- (1) Gao, J. *J. Phys. Chem. B* **1997**, *101*, 657.
- (2) Gao, J. *J. Chem. Phys.* **1998**, *109*, 2346.
- (3) Xie, W.; Gao, J. *J. Chem. Theory Comput.* **2007**, *3*, 1890.
- (4) Xie, W.; Song, L.; Truhlar, D. G.; Gao, J. *J. Chem. Phys.* **2008**, *128*, 234108.
- (5) Song, L.; Han, J.; Lin, Y. L.; Xie, W.; Gao, J. *J. Phys. Chem. A* **2009**, *113*, 11656.
- (6) Wierzchowski, S. J.; Kofke, D. A.; Gao, J. *J. Chem. Phys.* **2003**, *119*, 7365.
- (7) Xie, W.; Song, L.; Truhlar, D. G.; Gao, J. *J. Phys. Chem. B* **2008**, *112*, 14124.
- (8) Xie, W.; Orozco, M.; Truhlar, D. G.; Gao, J. *J. Chem. Theory Comput.* **2009**, *5*, 459.
- (9) Cembran, A.; Bao, P.; Wang, Y.; Song, L.; Truhlar, D. G.; Gao, J. *J. Chem. Theory Comput.*, accepted; DOI: 10.1021/ct100268p.
- (10) Mo, Y.; Peyerimhoff, S. D. *J. Chem. Phys.* **1998**, *109*, 1687.
- (11) Mo, Y.; Gao, J.; Peyerimhoff, S. D. *J. Chem. Phys.* **2000**, *112*, 5530.
- (12) Mo, Y.; Zhang, Y.; Gao, J. *J. Am. Chem. Soc.* **1999**, *121*, 5737.

- (13) Stoll, H.; Wagenblast, G.; Preuss, H. *Theor. Chim. Acta* **1980**, *57*, 169.
- (14) Mo, Y.; Song, L.; Lin, Y. *J. Phys. Chem. A* **2007**, *111*, 8291.
- (15) Mo, Y.; Gao, J. *J. Phys. Chem. A* **2001**, *105*, 6530.
- (16) Mo, Y.; Subramanian, G.; Gao, J.; Ferguson, D. M. *J. Am. Chem. Soc.* **2002**, *124*, 4832.
- (17) Mo, Y.; Schleyer, P. v. R.; Wu, W.; Lin, M.; Zhang, Q.; Gao, J. *J. Phys. Chem. A* **2003**, *107*, 10011.
- (18) Cubero, E.; Luque, F. J.; Orozco, M.; Gao, J. *J. Phys. Chem. B* **2003**, *107*, 1664.
- (19) Brauer, C. S.; Craddock, M. B.; Kilian, J.; Grumstrup, E. M.; Orilall, M. C.; Mo, Y.; Gao, J.; Leopold, K. R. *J. Phys. Chem. A* **2006**, *110*, 10025.
- (20) Mo, Y.; Gao, J. *J. Phys. Chem. B* **2006**, *110*, 2976.
- (21) McWeeny, R. *Proc. R. Soc. London, A* **1959**, *253*, 242.
- (22) Stoll, H.; Preuss, H. *Theor. Chem. Acc.* **1977**, *46*, 12.
- (23) Shukla, A.; Dolg, M.; Stoll, H.; Fulde, P. *Chem. Phys. Lett.* **1996**, *262*, 213.
- (24) Hankins, D.; Moskowitz, J. W.; Stillinger, F. H. *J. Chem. Phys.* **1970**, *53*, 4544.
- (25) Zhang, D. W.; Xiang, Y.; Zhang, J. Z. H. *J. Phys. Chem. B* **2003**, *107*, 12039.
- (26) Ding, Y.; Mei, Y.; Zhang, J. Z. H. *J. Phys. Chem. B* **2008**, *112*, 11396.
- (27) Cembran, A.; Song, L.; Mo, Y.; Gao, J. *J. Chem. Theory Comput.* **2009**, *5*, 2702.
- (28) Gao, J.; Garcia-Viloca, M.; Poulsen, T. D.; Mo, Y. *Adv. Phys. Org. Chem.* **2003**, *38*, 161.
- (29) Gao, J.; Mo, Y. *Prog. Theor. Chem. Phys.* **2000**, *5*, 247.
- (30) Mo, Y.; Gao, J. *J. Comput. Chem.* **2000**, *21*, 1458.
- (31) Mo, Y.; Gao, J. *J. Phys. Chem. A* **2000**, *104*, 3012.
- (32) Song, L.; Gao, J. *J. Phys. Chem. A* **2008**, *112*, 12925.
- (33) Song, L.; Mo, Y.; Gao, J. *J. Chem. Theory Comput.* **2009**, *5*, 174.
- (34) Song, L.; Mo, Y.; Zhang, Q.; Wu, W. *J. Comput. Chem.* **2005**, *26*, 514.
- (35) Nadig, G.; Van Zant, L. C.; Dixon, S. L.; Merz, K. M., Jr. *J. Am. Chem. Soc.* **1998**, *120*, 5593.
- (36) Van der Vaart, A.; Merz, K. M., Jr. *J. Phys. Chem. A* **1999**, *103*, 3321.
- (37) Van der Vaart, A.; Merz, K. M., Jr. *J. Am. Chem. Soc.* **1999**, *121*, 9182.
- (38) Van Der Vaart, A.; Merz, K. M., Jr. *Int. J. Quantum Chem.* **2000**, *77*, 27.
- (39) van der Vaart, A.; Merz, K. M., Jr. *J. Chem. Phys.* **2002**, *116*, 7380.
- (40) Bryantsev, V. S.; Diallo, M. S.; van Duin, A. C. T.; Goddard, W. A. I. *J. Chem. Theory Comput.* **2009**, *5*, 1016.
- (41) Chen, W.; Gordon, M. S. *J. Phys. Chem.* **1996**, *100*, 14316.
- (42) Kitaura, K.; Morokuma, K. *Int. J. Quantum Chem.* **1976**, *10*, 325.
- (43) Mo, Y.; Wu, W.; Song, L.; Lin, M.; Zhang, Q.; Gao, J. *Angew. Chem., Int. Ed.* **2004**, *43*, 1986.
- (44) Song, L.; Song, J.; Mo, Y.; Wu, W. *J. Comput. Chem.* **2009**, *30*, 399.
- (45) Mo, Y.; Gao, J. *Acc. Chem. Res.* **2007**, *40*, 113.
- (46) Cembran, A.; Payaka, A.; Lin, Y. L.; Xie, W.; Song, L.; Mo, Y.; Gao, J. *J. Chem. Theory Comput.* **2010**, *6*, 2242.
- (47) King, H. F.; Staton, R. E.; Kim, H.; Wyatt, R. E.; Parr, R. G. *J. Chem. Phys.* **1967**, *47*, 1936.
- (48) Schmidt, M. W.; Baldridge, K. K.; Boatz, J. A.; Elbert, S. T.; Gordon, M. S.; Jensen, J. H.; Koseki, S.; Matsunaga, N.; Nguyen, K. A.; Su, S. J.; Windus, T. L.; Dupuis, M.; Montgomery, J. S. *J. Comput. Chem.* **1993**, *14*, 1347.
- (49) Woon, D. E.; Dunning, T. H., Jr. *J. Chem. Phys.* **1995**, *103*, 4572.
- (50) Chirgwin, H. B.; Coulson, C. A. *Proc. R. Soc. London, Ser. A* **1950**, *2*, 196.
- (51) Schutz, M.; Burgi, T.; Leutwyler, S.; Burgi, H. B. *J. Chem. Phys.* **1993**, *99*, 5228.
- (52) Mulliken, R. S. *J. Chem. Phys.* **1964**, *61*, 20.
- (53) Gao, J.; Xia, X. *Science* **1992**, *258*, 631.

CT100292G